



JAAS

**Lithium isotopic analysis by quadrupole-ICP-MS:  
Optimization for geological samples**

Journal:	<i>Journal of Analytical Atomic Spectrometry</i>
Manuscript ID	JA-ART-05-2019-000175.R1
Article Type:	Paper
Date Submitted by the Author:	15-Jun-2019
Complete List of Authors:	Liu, Xiao-Ming; University of North Carolina at Chapel Hill, Geological Sciences Li, Wenshuai; University of North Carolina at Chapel Hill, Geological Sciences

SCHOLARONE™  
Manuscripts

1  
2  
3 **Optimization of lithium isotopic analysis in geological materials by**  
4 **quadrupole ICP-MS**  
5  
6  
7  
8  
9

10 Xiao-Ming Liu\* and Wenshuai Li\*

11  
12 Department of Geological Sciences, University of North Carolina-Chapel Hill, NC, USA  
13  
14  
15  
16  
17  
18  
19  
20

21 \*Corresponding author contact information:  
22

23 Plasma Mass Spectrometry Laboratory  
24

25 University of North Carolina at Chapel Hill  
26

27 104 South Road, Mitchell Hall  
28

29 Chapel Hill, NC 27599-3315  
30

31 Tel: (919) 962-0675  
32

33 Email: [xiaomliu@unc.edu](mailto:xiaomliu@unc.edu) & [wenshuai@live.unc.edu](mailto:wenshuai@live.unc.edu)  
34  
35  
36  
37  
38

39 Word count for the main text is 4606  
40  
41

42 6 Figures and 4 Tables  
43  
44  
45  
46  
47  
48  
49  
50  
51  
52  
53  
54  
55  
56  
57  
58  
59  
60

**Abstract:** This study develops and optimizes a new protocol to measure lithium isotope ratios using a single collector quadrupole inductively-coupled plasma mass spectrometer (Q-ICP-MS) operated in hot plasma (1550 W) conditions with sample-standard bracketing method. Our Q-ICP-MS method reduces sample consumption to 2.5 ng Li and achieves high long-term precision of 1.1‰ (2SD). This Q-ICP-MS method exhibits high matrix tolerance ( $\text{Na/Li} < 100$ ), suitable for ng-sized and high-matrix geological samples. We also developed a dual-column system for Li separation, with large loading capacity (29.6 meq), complete recovery ( $\sim 100\%$ ) and satisfactory purification ( $\text{Na/Li } m/m < 1$ ), as well as a fixed elution range for Li fractions (28-60 ml). This new chromatography method has been applied to chemically-diverse materials, producing consistent results. In addition, we report the Li isotopic compositions of 13 geostandards, and our measurements agree well with reported data within analytical uncertainties. This study documents that Li elemental concentration and Li isotope composition can be routinely measured using a single collector ICP-MS, which is convenient and commercially affordable for future Li isotope research across the fields of Earth and Environmental Sciences.

**Keywords:** Li isotopes; matrix effect, dual-column; Q-ICP-MS; geostandards.

## Introduction

Recent studies have advanced our knowledge of lithium (Li) isotope geochemistry by documenting the Li isotopic variations among geological reservoirs on Earth, and other bodies in the solar system<sup>1-4</sup>. Knowledge of Li isotope systematics provides a new tracer to understand various geological processes, as silicate weathering<sup>5-7</sup>, hydrothermal alteration<sup>8-11</sup>, metamorphic dehydration<sup>12-14</sup>, temperature-driven diffusion<sup>15-17</sup> and source mixing<sup>18-20</sup>. Precise and accurate determination of Li isotope compositions in geological samples is crucial to expanding the application of Li isotopes. High-precision Li isotope measurement are usually performed on thermal ionization mass spectrometry (TIMS,  $2\text{SD} = \pm 0.08 \sim 2.5\%$ )<sup>21-24</sup> and multicollector inductively coupled plasma mass spectrometer (MC-ICP-MS,  $2\text{SD} = \pm 0.2 \sim 1.4\%$ )<sup>25-31</sup>. However, these methods are susceptible to matrix-driven ionization suppression<sup>32</sup>. To minimize matrix-induced mass bias effects, previous studies highlighted complete separation of Li from interfering elements<sup>33-35</sup>. Besides, TIMS and MC-ICP-MS techniques have multiple limitations. For example, TIMS methods usually require large sample consumption ( $> 100$  ng Li), with high procedural blanks (100 pg level Li) and instrumental fractionation<sup>23-24</sup>. Comparatively, MC-ICP-MS methods show low-mass requirement ( $\sim 2-40$  ng Li)<sup>25-30</sup>, but are sensitive to matrix interferences<sup>36-37</sup>. Moreover, low-level resistors of the faraday cups exhibit low ion detection sensitivity, which is challenging for samples with super-low analyte concentration and high matrix<sup>25-27</sup>.

Early application of quadrupole inductively-coupled plasma mass spectrometer (Q-ICP-MS) demonstrated small sample requirement (down to 5 ng Li) and acceptable precision ( $2\text{SD} = \pm 1.0\%$  at best)<sup>38-40</sup>. Since the development of MC-ICP-MS in the first decade of the 21<sup>st</sup> century, few efforts have been focused on Q-ICP-MS. Thus, the most recent endeavor has been made by Misra and Froelich (2009)<sup>42</sup>. Their method employed an older version of the Q-ICP-MS (Agilent<sup>TM</sup> 7500), and used cool plasma conditions for Li isotopic analysis. They achieved sub-ng level Li requirement and high external precision ( $2\text{SD} = \pm 1.5\%$ ) for seawater and natural carbonate samples. Since the instrument used is out of production, development and optimization of new Q-ICP-MS instrument platform is needed. Moreover, a routine analytical method is important for the wider application of Li isotopes across the fields of Earth and Environmental Sciences.

Here we refine the Li column chemistry, and develop a simple analytical routine using an Agilent™ 7900 Q-ICP-MS for Li isotopic analysis. Our chromatographic protocol aims to achieve low blank, high loading capacity, 100 % yield, and fixed Li elution range. The instrumental setup developed has been optimized and confirmed to achieve high-precision Li isotope measurement ( $2SD=\pm 1.1\%$ ) with low-mass requirement. Our objective is to provide operational guidance for scientists interested in Li isotope measurements through a convenient and commercially affordable way.

## Materials and methods

All the experimental and analytical work in this study was conducted in the Plasma Mass Spectrometry (PMS) Lab at the University of North Carolina, Chapel Hill. Sample dissolution and column chemistry were done in class 100 vertical laminar flow hoods. A full description of the proposed protocols and analysis techniques is given as follows.

### Chemicals and standards

Ultrapure water (18.2 MΩ) was produced by de-ionization of reverse osmosis water using a Milli-Q water purification system (Direct-Q 3 UV, Merck Millipore™, Germany). High-purity nitric acid (HNO<sub>3</sub>), hydrochloric acid (HCl) and hydrofluoric acid (HF) were purified in-house with double distillation in Savillex™ Teflon acid purification systems. Acids used were gravimetrically diluted to required molarities with MQ water. Lithium isotopic standards IRMM-016<sup>42</sup>, available from the Institute for Reference Materials and Measurements (IRMM), was used as the bracketing standard.

For optimization of the isolation of lithium from various geological samples, 13 certified international reference materials with different Li contents and matrix/Li ratios are adopted in this study to evaluate the effect of matrix on column chemistry. The geostandards covering a large range of chemically-diverse geological materials were processed and analyzed to assess the accuracy and procedural reproducibility. We purchased a limestone standard (NIST-SRM-1d) from the National Institute of Standards and Technology, a coral standard (JCP-1) from the Geological Survey of Japan, a granodiorite (GSP-2), a continental flood basalt (BCR-2), an ocean island basalt (BHVO-2), a marine manganese nodule (NOD-A-1) and a marine shale (SBC-1) from the United States Geological Survey. We also obtained a basalt standard (JB-2) and a granite standard (JG-2) from the Geological Survey of Japan. In addition, we purchased three clay standards (kaolinite, KGa-2; illite, IMt-2, montmorillonite, SWy-3) from the Clay Mineral Society and a seawater standard (NASS-7) from the National Research Council Canada. These standards have been widely used in Li isotope research and thus permit inter-laboratory comparisons.

### Sample digestion

The entire sample digestion was performed at the Isotope Geochemical Laboratory at the University of North Carolina, Chapel Hill. Between 10 and 100 mg of standard powders were acid-digested with the HF-HNO<sub>3</sub> mixture (3:1 v/v) in 15 ml Savillex™ Teflon beakers and put on the hotplate at temperatures exceeding 120 to 130 °C until total dissolution was achieved. The shale standard SBC-1 was treated with ultrapure H<sub>2</sub>O<sub>2</sub> (Fisher Scientific™) to oxidize the organics. Samples were then dried down, refluxed with *aqua regia* (3:1 M/M; conc. HNO<sub>3</sub>: conc. HCl) and put on hotplate at ~120 °C overnight. The drying operation was repeated, using the same amount of HCl until the solution became clear. After dryness, acquired residues were dissolved in 2% (v/v) nitric acid. All prepared samples stored in class 100 vertical laminar flow hoods (AirClean™ 600

1  
2  
3 PCR workstation). Acquired samples were dried down and re-dissolved in 0.7 M HNO<sub>3</sub>, and ready  
4 for column chemistry.  
5

### 6 **Chromatography**

7 For precise Li isotope measurement, it is crucial to thoroughly separate Li from other matrix  
8 elements, because the presence of matrix elements could generate spectral effects on Li isotopes.  
9 The common peak overlap in chromatography, making quantitative separation of Li from Na  
10 analytically challenging<sup>35</sup>. To ensure the matrix-matched principle on Li isotopic measurement,  
11 Na should also be separated from Li, in particular for low sample size and high-matrix level  
12 geological samples (e.g., seawater and brines). Designed chromatography was composed of two  
13 steps to ensure high sample loading and fixed Li elution range (Table 1). The first steps were made  
14 using BioRad™ Econo-Pac (1.5 cm ID, polypropylene) and the second steps were custom-made  
15 (0.6 cm ID, polypropylene) columns. All columns were loaded with pre-cleaned cation-exchange  
16 resin, AG 50W-X8 resin (200-400 mesh size), which was successfully used to separate Li and K  
17 from natural samples<sup>28-29, 42-44</sup>.  
18  
19

20  
21 Our column protocol includes two steps which allows Li to be isolated sufficiently from the  
22 matrices, with special optimization for ng-sized and high-matrix level geological samples. The  
23 main differences between this study and our previous study<sup>35</sup> are the size of polypropylene column  
24 and the volume of the resin. The first step for purifying Li with partial Na from most major and  
25 minor elements with 0.7 M HNO<sub>3</sub> through the fat column loaded with 17 mL resin. So, the total  
26 capacity of the wet resin is 29.6 meq (1.74 meq/ml wet capacity). This capacity meets the  
27 requirement for Li separation from geological samples with diverse matrix compositions. Columns  
28 were first cleaned with 100 mL 6 mol l-1 double-distilled HCl and then conditioned with 50 mL  
29 0.7 mol/L double-distilled HNO<sub>3</sub>. After centrifuging, samples dissolved in 2 mL 0.7 mol/L HNO<sub>3</sub>  
30 were loaded onto the first columns. Matrix elements were eluted by adding 25 mL 0.7 mol HNO<sub>3</sub>  
31 and then pre-cuts were collected into acid-cleaned polypropylene tubes by adding 5 mL 0.7 mol/L  
32 HNO<sub>3</sub>. Li fractions were recovered into acid-cleaned Teflon beakers using 50 mL 0.7 mol/L HNO<sub>3</sub>.  
33 Post-cuts were also collected into additional acid-cleaned polypropylene tubes with 5 mL 0.7  
34 mol/L HNO<sub>3</sub>. The recovered Li was then dried down and dissolved with 2 mL 0.2 mol/L HCl  
35 before loading onto the second column. The second column for separating Li from Na with 0.2 M  
36 HCl through the thin column packed with 3.4 mL resin.  
37  
38  
39

40 All columns were first cleaned with 50 mL 6 mol/L double-distilled HCl and then conditioned  
41 with 20 mL 0.2 mol/L HCl. The samples in 2 ml 0.2 mol/L HCl were loaded onto the second  
42 columns. Matrix elements were eluted by adding 30 mL 0.2 mol/L HCl and pre-cuts were collected  
43 into acid-cleaned polypropylene tubes with 2 mL 0.2 mol/L HCl. Subsequently, Li was recovered  
44 into acid-cleaned Teflon beakers using 28 mL 0.2 mol/L HCl. Post-cuts were collected into  
45 additional acid-cleaned polypropylene tubes by adding 2 mL 0.2 mol/L HCl. The recovered Li  
46 solutions were dried down and turned to the nitrate matrix form. Afterward, aliquots of each  
47 samples were prepared in 2% HNO<sub>3</sub> (v/v) containing 0.5 ppb Li for Q-ICP-MS analyses. The total  
48 procedure blank is <0.004 ng. The final Na/Li (*m/m*) in collections is less than 1, preventing the  
49 potential interference of Na<sup>+</sup> on Li isotope analysis.  
50  
51

### 52 **Mass spectrometry**

53 All isotope analyses were performed using an Agilent Technologies™ 7900, a single collector  
54 quadruple-ICP-MS at the Plasma Mass Spectrometry Laboratory (PMS) at the University of North  
55 Carolina, Chapel Hill. The instrumental settings for Li isotope ratio determination are summarized  
56  
57  
58  
59  
60

in Table 2, where both hot plasma (1550 W) and cool (600 W) plasma conditions were tested. We used an Agilent™ microflow self-aspirating 200 µl/min PFA nebulizer, quartz spray chamber, quartz torch and 2.5 mm internal diameter injector and S-lenses. We compared platinum and nickel cones and skimmers for carry over effects and blanks, but did not observe any difference. Therefore, we adopted nickel cones for all Li isotope analyses. To reach high signal stability and low background, we optimized the nebulizer and make up gas flow. To obtain equal numbers of ion counts for both Li isotopes, we used integration time of 1s and 12s for <sup>7</sup>Li and <sup>6</sup>Li, respectively, roughly in inverse proportion to their natural isotope abundance. All tuning parameters are checked daily to maximize instrument sensitivity and stability. Each measurement included 1000 integrations of <sup>7</sup>Li and <sup>6</sup>Li measurement and replicate between 5 and 8 times, followed by 3 minutes washing to lower the Li signal to an insignificant level (<100 cps on <sup>7</sup>Li). The instrumental sensitivity was on average 250, 000 cps on <sup>7</sup>Li for a 0.5 µg/L solution.

The discrepancy between measured and true Li isotope ratios may come from three factors: memory effects, instrumental mass bias, and matrix effects. Because of the low sample size (0.5 µg/L) and long washing time (180 s) adopted as the control of background levels, memory effects can be sufficiently mitigated. In particular, we used three washing reagents to ensure thorough washout of Li: (i) 1% HF+2% HNO<sub>3</sub> (v/v), (ii) 1% HNO<sub>3</sub>+5% HCl (v/v) mixture, and (iii) 2% HNO<sub>3</sub> (v/v). Compared with the 2% HNO<sub>3</sub>-only washing method, the blank was significantly decreased when adding 1% HF+2% HNO<sub>3</sub> and 2% HNO<sub>3</sub>+5% HCl. The blank signals for <sup>7</sup>Li (<10 CPS, 0.1s integration) were orders of magnitude lower compared with 2% HNO<sub>3</sub>-only washing procedure, which lowered analytical uncertainties for our isotope ratios. Commonly, the plasma-source mass spectrometry suffers from instrumental mass bias derived from preferential extraction and transmission of heavier ions over lighter ions<sup>41</sup>. We observed slight instrumental drifts in <sup>7</sup>Li/<sup>6</sup>Li ratios with time (not shown here). So, we used by standard-sample-standard bracketing protocol to acquire precise Li isotope data. Here we express the Li isotopic composition using δ<sup>7</sup>Li, which is the per mil deviation from the NIST L-SVEC standard, defined as δ<sup>7</sup>Li (‰, L-SVEC) = [(<sup>7</sup>Li/<sup>6</sup>Li)<sub>Sample</sub> / (<sup>7</sup>Li/<sup>6</sup>Li)<sub>L-SVEC</sub> - 1] × 1000. While L-SVEC is no longer available and the IRMM-016 standard show identical Li isotopic composition. Therefore, we used IRMM-016 as the bracketing standard to correct for instrumental mass bias. After this correction and thorough washout between samples, the remaining δ<sup>7</sup>Li drifts on Q-ICP-MS could be attributed to matrix effects, which will be evaluated in details next.

## Results and discussion

### Generalized chromatographic purification

Various single- and dual-column cation-exchange chromatography have been described in the literature for Li isotope analysis<sup>25,27-30,33-34,47-48</sup>. However, the application of single-column separation of Li can be largely limited by high cumulative procedural blanks, the tailing of Li peaks, and incomplete Li recovery and subsequent column-induced isotopic fractionation<sup>42</sup>. To achieve satisfactory Li/matrix elements separation, large resin loads, high aspect ratios, and large eluent volumes are required<sup>3</sup>. In addition, significant Li peak migrations generally occur due to changes in matrix load and elution matrix strength. Here we are using a modified dual-column procedure to achieve fixed Li elution peaks with complete separation from matrix Na. Using 0.7 mol/L HNO<sub>3</sub> elution acid in the first step columns, high ionic potential cations such as Fe<sup>3+</sup> and Al<sup>3+</sup> are retained by the resin, but low ionic potential cations (i.e., Li<sup>+</sup>, Na<sup>+</sup> and K<sup>+</sup>) with low partition coefficients directly go through. Li is the first element to elute off from the columns during 30 to 80 ml elution acid within 50 ml of total elution volume (Fig. 1). Both pre-cuts and

1  
2  
3 post-cuts have negligible amount of Li. Sodium, the next element to elute after Li, presents after  
4 52 ml of elution. Not surprisingly, a complete separation between lithium and sodium cannot be  
5 achieved with the first column, requiring the second column for further purification of Li from Na.  
6 Using 0.2 mol/L HCl in the second chromatographic step, Li fractions are in the 32 to 60 ml elution  
7 fraction within 28 ml of total elution volume, completely separated from Na. Low blanks of both  
8 pre-Li and post-Li fractions demonstrate the absence of Li breakthrough or tailing of elution peaks.  
9

10  
11 The compositionally-diverse geological samples yield analogous elution curves (Fig. 1),  
12 proving that this method is widely suitable to samples with various matrix compositions. In  
13 comparison with single-column systems, the most significant advantage of this dual-column  
14 system is the high loading capacity for low-Li samples and consistent elution range of the Li cuts  
15 for geomaterials with various matrix compositions, eliminating the need for repeated  
16 chromatography, material-specific column systems<sup>33</sup> and elution curve recalibration<sup>3</sup>. The low  
17 cumulative Li blank, high loading capacity and fixed Li elution range are key features of our  
18 method, particularly suitable for low-Li sized and high-matrix geological samples. The Li yields  
19 of samples after column chemistry can be determined by collecting pre- and after-cuts in addition  
20 to Li cuts. We have checked our Li column yields by comparing Li cuts to the sum of Li cuts, and  
21 pre- and after-cuts to ensure ~100% Li recovery (Table 3).  
22  
23

## 24 **Precision and accuracy**

### 25 *Short-term and long-term stability*

26 Precision and accuracy of our analytical procedure were evaluated by repeated analyses of pure  
27 Li reference solutions (IRMM-016), as well as two USGS rock standards (BCR-2 and JG-2). To  
28 account for the instrument drift, mass bias, short-term examination bracketed by IRMM-016 Li  
29 standard was performed. As discussed above, we measured each sample 5-8 times and reported  
30 the averages of repeat measurements. The short-term stability (2SD) of the Q-ICP-MS method are  
31 1.6‰ for IRMM-016 solution, 1.1‰ for BCR-2 basalt standard and 1.7‰ for JG-2 granite  
32 standard, respectively. To evaluate the long-term reproducibility, two geostandards BCR-2 and  
33 JG-2 in addition to the IRMM-016 standard were routinely measured over a period of 10 months  
34 (Fig. 2). During the 10-month period from April, 2018 to January, 2019, the averaged  $\delta^7\text{Li}$  was 3.1‰  
35 for BCR-2 and 0.2‰ for JG-2, with the long-term external two standard deviation (2SD) of 1.1‰  
36 and 1.0‰, respectively. We take the 2SD range from these long-term standard analyses as a  
37 representative value for the bracketing standards during one analytical session. Based on these  
38 results, the long-term external reproducibility of our analytical routine is conservatively estimated  
39 to be better than 1.1‰, comparable to a recent MC-ICP-MS study of 1.1‰<sup>49</sup>.  
40  
41  
42

### 43 *Application to the reference materials*

44 The whole-procedure accuracy of our analytical routine can be validated by comparable results  
45 obtained between our and other laboratories for 13 chemically-diverse natural geological standards  
46 with different matrix compositions (Table 4). In addition, we also report the Li isotopic data of  
47 IRMM-016 after column chemistry to validate our chromatography method. The results from three  
48 basaltic references BHVO-2 ( $4.7 \pm 0.57\%$ ,  $n=10$ ), BCR-2 ( $3.16 \pm 1.10\%$ ,  $n=10$ ), JB-2 ( $4.56 \pm 0.56\%$ ,  
49  $n=10$ ), are consistent with published data, within the analytical error. The average  $\delta^7\text{Li}$  values  
50 measured for two granitic standards JG-2 ( $0.25 \pm 1.02\%$ ,  $n=54$ ) and GSP-2 ( $-0.56 \pm 0.72\%$ ,  $n=54$ )  
51 are in agreement with published data<sup>6,27,34-35,50-51</sup>. The carbonate standard JCP-1 yields  $\delta^7\text{Li}$  values  
52 of  $19.83 \pm 1.07\%$  ( $n=10$ ), which are slightly lower than the reported data ( $20.16-20.27\%$ )<sup>29,31</sup>, but  
53 within uncertainty. Clay Swy-3 (smectite), KGa-2 (kaolinite) and IMt-2 (illite) presents  $\delta^7\text{Li}$  values  
54  
55  
56  
57  
58  
59  
60

of  $-0.58 \pm 0.36\%$  (n=10),  $0.16 \pm 0.69\%$  (n=10) and  $5.95 \pm 0.68\%$  (n=10). These results are consistent with the reported data<sup>18</sup>. The Li isotopic compositions in three sedimentary geostandards, carbonate NIST-SRM-1d, manganese nodule NOD-A-1 and shale SBC-1 are  $6.07 \pm 1.20\%$  (n=10),  $26.85 \pm 1.30\%$  (n=10) and  $0.23 \pm 0.90\%$  (n=10) respectively, agreeing well with our previous study (i.e., SBC-1,  $5.63 \pm 0.48\%$ , n=4; NOD-A-1,  $0.29 \pm 0.23\%$ , n=3)<sup>35</sup>.

Because of the long residence time in the open ocean ( $\sim 1.5$  Ma)<sup>50</sup> compared to the ocean mixing time ( $\sim 1$  kyr), Li is a conservative element with homogeneous elemental and isotopic compositions<sup>23,53-54</sup>. Using a Q-ICP-MS instrument, Misra and Froelich (2009)<sup>42</sup> reported an overall seawater  $\delta^7\text{Li}$  ratio of  $30.75 \pm 0.41\%$  (n=10), identical to the average published value of  $31.0 \pm 0.5\%$ .<sup>2</sup> In this study, the seawater standard NASS-7 yields average  $\delta^7\text{Li}$  of  $30.42 \pm 0.97\%$  (n=3), consistent with our recent work using a MC-ICP-MS<sup>35</sup> and the published seawater standards NASS-5 and NASS-6 values ( $29.6$ - $30.87\%$ ).<sup>28-30,34,55-56</sup> In addition, an aliquot of the Li standard solution (IRMM-016) was processed through column chemistry, whose  $\delta^7\text{Li}$  values ( $0.16 \pm 0.83\%$ ) agreed with our long-term average value of  $0.15\%$  (Fig. 2) without column within our precision. To establish the validity of this method, the values obtained from separately digested materials in different measurement sessions over a period of ten months by our Q-ICP-MS method also confirm a long-term consistency and external reproducibility. In summary, there is no systematic shift found between data from Q-ICP-MS (this study), TIMS and MC-ICP-MS from different laboratories (Table 4). Therefore, we listed the measured data in this study as acceptable reference values, and recommend for future inter-laboratory comparison.

### Optimization of Li isotopic analysis

This section provides detailed information on how to achieve routine high precision and accuracy Li isotopic analysis using a Q-ICP-MS through optimization of various parameters.

#### *RF power: hot plasma vs. cool plasma*

The choice of *PF* power reflects a balance between the ionization efficiency and amount of interferences. Previous studies have adopted two plasma powers to achieve high precision Li isotope analysis: cool plasma<sup>42</sup> and hot plasma condition<sup>40</sup>. The major advantage of cool plasmas conditions is that lithium with low first ionization potential is almost completely ionized while formation of oxides and doubly charged ion formation are minimized. Moreover, in cool plasma conditions ionization of other matrix-based high first ionization potential interferences is significantly reduced. The hot plasma conditions have the advantage of higher plasma stability and sensitivity. Therefore, we tested cool plasma (600 W) and hot plasma (1550 W) conditions to optimize *PF* power for Li isotope analysis. We tuned the ICP-MS to maximize lithium sensitivity and signal stability in both cool and hot plasma settings, respectively.

Comparing with the cool plasma conditions, the hot plasma settings demonstrate better external precision of  $\pm 1.1\%$  (2SD) (Fig. 3). The possible reason may be the accurate Li isotope ratio determination by ICP-MS is sensitive to the presence of matrix elements, especially in the cold plasma<sup>26</sup>. To minimize the plasma-based argon ionization in the central channel and doubly charged  $^{12}\text{C}^{2+}$  and  $^{14}\text{N}^{2+}$  interferences on  $^6\text{Li}^+$  and  $^7\text{Li}^+$ , Misra and Froelich (2009)<sup>42</sup> used cool plasma conditions (600 W) with an Agilent<sup>TM</sup> 7500 Q-ICP-MS. Cool plasma has its advantages because of its lower background for Li. However, oxides are usually high in cool plasma condition, creating possible matrix effects.



### *Acid molarity matching*

The uncertainty associated with differences in the molarity of concentrated acids, volume and weight measurements, as well as occasional artifacts (e.g., operation miss and evaporation) may change final acid molarity. The mismatch in acid molarity between samples and bracketing standards could introduce significant shifts in space charge effects. Such influence could cause differential instrumental mass bias between samples and their bracketing standards, resulting in measurable difference in isotopic ratios. These offsets have been observed for K, Mg and Fe isotope systems<sup>56-58</sup>. The effect of such a mismatch on Li isotopic analysis by Q-ICP-MS has not, to our knowledge, been reported. To test possible impacts of acid mismatch on Li isotopic analysis, pure IRMM-016 solutions of 0.5 ppb Li in 1-5% HNO<sub>3</sub> (v/v) against the same solutions in 2% HNO<sub>3</sub> (v/v). Interestingly, the results demonstrated a positive correlation between the  $\delta^7\text{Li}$  values of the sample and how well its concentration matches the bracketing standard (Fig. 4). The 0.5ppb IRMM-016 in 2% HNO<sub>3</sub> (v/v) solutions bracketed by themselves yielded  $\delta^7\text{Li}$  values between -0.01‰ and 0.01‰, consistent with the expected value of 0 ‰. However, both low and high acid molarity with respect to the bracketing solutions led to large drifts, up to ~8 ‰ in Li isotopic analysis. Our tests on Q-ICP-MS showed that acid mismatches can significantly affect the accuracy of Li isotopic analysis. As such, one needs to match the acid molarity of samples and standards.

### *Concentration matching*

Instrumental mass bias could be significant and fluctuate with time, thus reducing the accuracy and precision of isotopic measurement. Here standard-sample bracketing method was used by assuming instrumental mass bias for sample and standard is the same. This requires that the sample and standard have identical Li concentrations. First, we tested the lower Li threshold of isotopic measurement for the optimization of low-size samples. Apparently, the Li concentration selection of with a range of 0.1-5 ppb can introduce small, but measurable errors in Li isotope data acquisition by Q-ICP-MS (Fig. 5). The isotopic response to increasing Li concentration is invariant in the 0.5 ppb to 5 ppb range, within the external precision (2SD=±1.1‰). This amount of Li required for a single Q-ICP-MS analysis (0.5 ng) is almost an order of magnitude less than required by previous MC-ICP-MS methods<sup>25-28,54</sup>. There is a decreasing stability of Li isotope analysis with Li concentration down to 0.1-0.25 ppb, probably due to the insufficient detection sensitivity.

Li concentration mismatch between the sample and its bracketing standards may influence the accuracy of Li isotope analysis. Such effects on Li isotope measurement were evaluated by testing Li concentration mismatched (between 80 and 150%) IRMM-016 standards bracketed with the same 0.5 ppb Li standard. The results depicted in Fig. 5 demonstrate systematic  $\delta^7\text{Li}$  offsets for mismatches in Li concentration between samples and standards. According to our results, Li concentration mismatch would result in observable deviation when the sample and standard concentration mismatch to be more than 10%. Therefore, we recommend that Li concentrations in samples and standards need to be matched within 5% to guarantee precision and accuracy.

### *Evaluation of matrix effects*

The matrix effect of Na (the most common matrix element) on Li isotopic analysis is evaluated, which could change the instrumental mass bias, violating the prerequisite for applying the standard sample-standard bracketing method<sup>25</sup>. Due to the small differences in the partition coefficients between Li and Na, the tailing of Na peaks in Li fractions is common during column purification, especially for those Na-enriched geological samples like seawater and brines. Therefore, two-step

1  
2  
3 chromatographic separation is commonly adopted for Li purification from matrix elements,  
4 especially for Na<sup>35</sup>. Nonetheless, we investigated the presence of Na on Li isotope measurements.  
5 Systematic investigations on Li isotope measurement techniques documented that significant  
6 interference of Na in sample solutions degrade the accuracy of Li isotope composition  
7 determinations, and are shown in Fig. 6. Generally, matrix-induced mass bias (Na/Li=20) can  
8 cause decrease in  $\delta^7\text{Li}$  values by up to 3‰<sup>27,47</sup>, potentially related to peak ionization delay<sup>26</sup>. In  
9 contrast, both Bryant et al. (2003)<sup>26</sup> and our recent work<sup>35</sup> demonstrated that high Na/Li ratios  
10 could induce  $\delta^7\text{Li}$  increase by  $\sim 1$ ‰. The increase in  $\delta^7\text{Li}$  due to high Na/Li ratio in the test solution  
11 is consistent with our current understanding of the space charged effects. With the presence of  
12 Na<sup>+</sup>, the light Li isotope (<sup>6</sup>Li<sup>+</sup>) should be preferentially expelled, thus increasing detected <sup>7</sup>Li/<sup>6</sup>Li  
13 ratios. It seems that spectral matrix effects could cause signal enhancement or suppression in  
14 different instrument settings, which is not a linear function of Na/Li (Fig. 6). Therefore, we  
15 speculate this deviation in  $\delta^7\text{Li}$  is complex, and may be linked to differences in various  
16 instrumental conditions.  
17  
18  
19

20 Complete removal of Na must be guaranteed for TIMS and MC-ICP-MS analyses. To examine  
21 the effect of Na on Li isotope measurement, we used a series of mixing solutions (0.5 ppb Li,  
22 IRMM-016) doped with various amount of Na (Na/Li mass ratios from 0.5 to 100). In contrast  
23 with results from MC-ICP-MS analysis, our results show that the presence of Na standards with  
24 Na/Li mass ratios up to 50 does not affect the accuracy of measured  $\delta^7\text{Li}$  values. A decrease in the  
25 measured  $\delta^7\text{Li}$  of 0.6‰ occur when Na/Li ratio reaches 100, although it is still within our reported  
26 analytical uncertainty of 2SD= $\pm 1.1$ ‰. High-resolution TIMS and MC-ICP-MS techniques require  
27 ultra-clean Li solutions to eliminate matrix-induced mass bias<sup>3</sup>. However, our results show large  
28 matrix tolerance of the Q-ICP-MS method. Thus, our Q-ICP-MS method with hot plasma is more  
29 resistant to matrix interferences. The Q-ICP-MS technique is more robust in terms of matrix  
30 tolerance compared to TIMS and MC-ICP-MS methods, especially for samples with high Na/Li  
31 ratios<sup>28,41</sup>. Therefore, if Na/Li ratios in samples are less than 100, column chemistry is unnecessary  
32 for the Q-ICP-MS approach designed.  
33  
34  
35

## 36 Conclusions

37 We have developed an efficient mass spectrometric protocol for routine and accurate  
38 determination of Li isotope ratios using an Agilent<sup>TM</sup> 7900 single collector Q-ICP-MS. The  
39 method shows comparable long-term precision (2SD= $\pm 1.1$ ‰,) and accuracy in comparison to  
40 TIMS and MC-ICP-MS techniques. Our analytical approach allows for low mass consumption  
41 (2.5 ng/quintuplicate analyses), low whole-procedure blank and high matrix tolerance (Na/Li  
42  $\sim 100$ ), pushing the boundary for Li isotope investigation of geological materials. We also  
43 presented a detailed dual-column Li purification protocol. This dual-column system has two  
44 advantages: (1) It enables high loading capacity (29.6 meq), complete recovery ( $\sim 100\%$ ) and  
45 satisfactory purification (Na/Li < 1) of Li. (2) The dual-column isolation routinely achieved a fixed  
46 elution range of Li cuts (32~60 ml 0.2 mol/L HCl), preventing re-calibration of columns for  
47 geologically diverse matrix variations. Furthermore, washing with 1% HF+2% HNO<sub>3</sub> (v/v), and  
48 then 1% HNO<sub>3</sub>+5% HCl (v/v), and 2% HNO<sub>3</sub> (v/v) in between analyses can significantly  
49 minimize the memory effect of Li. The newly-developed chromatography and Q-ICP-MS  
50 techniques can be applied to chemically-diverse materials, and is particularly optimized for ng-  
51 sized and high-matrix level geological samples such as seawater and brines. We reported accurate  
52 and reproducible Li isotope measurements in various geostandards, including seawater (NASS-7),  
53 igneous rocks (BHVO-2, BCR-2, JG-2, JB-2 and GSP-2), biogenetic/abiogenic carbonates  
54  
55  
56  
57

(IRMM-016, JCP-1 and NIST-SRM-1d), marine manganese nodule (NOD-A-1), shale (SBC-1) and clay minerals (KGa-2, IMt-2 and SWy-3). Our  $\delta^7\text{Li}$  results agree with published data, therefore our findings serve as reference values for quality control and inter-laboratory calibration.

## Conflicts of interest

There are no conflicts to declare.

## Author contribution

X-M. L. and W. L. contributed equally to this work.

## Acknowledgements

We would like to thank Bert Woods and Mark Kelinske for their help with the optimization of Q-ICP-MS for isotope analysis. Cheng Cao, Ryan Mills and Drew Coleman are thanked for their help at the Isotope Geochemistry Lab at UNC. The manuscript benefited from the comments of two anonymous reviewers and the efficient handling of the editor. We acknowledge funding support from NSF Career Award (EAR-1848153) and the University of North Carolina. This research is supported by the US Army Research Office under grant W911NF-17-2-0028. The views and conclusions contained in this document are those of the authors, and should not be interpreted as representing the official policies, either expressed or implied, of the sponsors, including the Army Research Laboratory or the U.S. Government. The U.S. Government is authorized to reproduce and distribute reprints for Government purposes notwithstanding any copyright notation herein.

## References

1. L.H. Chan, in *Handbook of Stable Isotope Analytical Techniques*, 2004, pp. 122-141.
2. P.B. Tomascak, in *Reviews in Mineralogy and Geochemistry*, 2004, pp.153-195.
3. P.B. Tomascak, T. Magna, and R. Dohmen, in *Advances in lithium isotope geochemistry*, 2016.
4. S. Penniston-Dorland, X.M. Liu and R.L. Rudnick, in *Reviews in Mineralogy and Geochemistry*, 2017, pp. 165-217.
5. Y. Huh, C.H. Chan and O.A. Chadwick, *Geochem. Geophys. Geosy.*, 2004, **5**, Q09002.
6. J.S. Pistiner, G.M. Henderson, *Earth Planet. Sci. Lett.*, 2003, **214**, 327-339.
7. R.L. Rudnick, P.B. Tomascak, H.B Njo and L.R. Gardner, *Chem. Geol.*, 2004, **212**, 45-57.
8. L.H. Chan and M. Kastner, *Earth Planet. Sci. Lett.*, 2000, **183**, 275-290.
9. R.H. James, D.E. Allen and W.E. Seyfried Jr, *Geochim. Cosmochim. Acta*, 2003, **67**,681-691.
10. C. Bouman, T. Elliott and P.Z. Vroon, *Chem. Geol.*, 2004, **212**, 59-79.
11. L.B. Williams,R.L. Hervig, *Geochim. Cosmochim. Acta*, 2005, **69**, 5705-5716.
12. L.D. Benton, J.G. Ryan and I.P. Savov, *Geochem. Geophys. Geosy.*, 2004, **5**, Q08J12.
13. F.Z. Teng, W.F. McDonough, R.L. Rudnick and B.A. Wing, *Chem. Geol.*, 2007, **239**, 1-12.

14. T. Zack, P.B. Tomascak, R.L. Rudnick, C. Dalpé and W.F. McDonough, *Earth Planet. Sci. Lett.*, 2003, **208**, 279-290.
15. C.C. Lundstrom, M. Chaussidon, A.T. Hsui, P. Kelemen and M. Zimmerman, *Geochim. Cosmochim. Acta*, 2005, **69**, 735-751.
16. F.M. Richter, A.M. Davis, D.J. vDePaolo and E.B. Watson. *Geochim. Cosmochim. Acta*, 2003, **67**, 3905-3923.
17. F.Z. Teng, W.F. McDonough, R.L. Rudnick and R.J., Walker, *Earth Planet. Sci. Lett.*, 2006, **243**, 701-710.
18. P.H. Tsai, C.F. You, K.F. Huang, C.H. Chung and T.B. Sun, *J. Asian Earth Sci.*, 2014, **87**, 1-10.
19. L. Sauzéat, R.L. Rudnick, C. Chauvel, M. Garçon and M. Tang, *Earth Planet. Sci. Lett.*, 2015, **428**, 181-192.
20. J.S. Harkness, N.R. Warner, A. Ulrich, R. Millot, W. Kloppmann, J.M. Ahad, M.M. Savard, P. Gammon and A. Vengosh, *Appl. Geochem.*, 2018, **90**, 50-62.
21. L. H. Chan, *Anal. Chem.*, 1987, **59**, 2662-2665.
22. T. Moriguti and E. Nakamura, *Proc. Jpn. Acad., Ser. B, Phys. Biol. Sci.*, 1993, **69**, 123-128.
23. C. F. You and L. H. Chan, *Geochim. Cosmochim. Acta*, 1996, **60**, 909-915.
24. T. Moriguti and E. Nakamura, *Chem. Geol.*, 1998, **145**, 91-104.
25. P. B. Tomascak, R. W. Carlson and S. B. Shirey, *Chem. Geol.*, 1999, **158**, 145-154
26. C. J. Bryant, M. T. McCulloch and V. C. Bennett, *J. Anal. At. Spectrom.*, 2003, **18**, 734-737
27. A. B. Jeffcoate, T. Elliott, A. Thomas and C. Bouman, *Geostand. Geoanal. Res.*, 2004, **28**, 161-172
28. M. Rosner, L. Ball, B. Peucker-Ehrenbrink, J. Blusztajn, W. Bach and J. Erzinger, *Geostand. Geoanal. Res.*, 2007, **31**, 77-88.
29. K.F. Huang, C.F. You, Y.H. Liu, R.M. Wang, P.Y. Lin and C.H. Chung, *J. Anal. At. Spectrom.*, 2010, **25**, 1019-1024.
30. M.S. Choi, J.S. Ryu, H.Y. Park, K.S. Lee, Y. Kil and H.S. Shin, *J. Anal. At. Spectrom.*, 2013, **28**, 505-509.
31. M.S. Bohlin, S. Misra, N. Lloyd, H. Elderfield and M.J. Bickle, *Rapid Commun. Mass Spectrom.*, 2018, **32**, 93-104.
32. D. Kutscher, J.D. Wills and S.M. Ducos, *Technical Note TN43202*, 2014, Bremen, Germany.
33. K. Van Hoecke, J. Belza, T. Croymans, S. Misra, P. Claeys and F. Vanhaecke, *J. Anal. At. Spectrom.*, 2015, **30**, 2533-2540.
34. J. Lin, Y. Liu, Z. Hu, L. Yang, K. Chen, H. Chen, K. Zong and S. Gao, *J. Anal. At. Spectrom.*, 2016, **31**, 390-397.

- 1
- 2
- 3 35. W.S. Li, X.M. Liu and L.V. Godfrey, *Geostand. Geoanal. Res.*, 2019. DOI: 10.1111/ggr.12254
- 4
- 5 36. J. Vogl, *Inductively Coupled Plasma Mass Spectrometry Handbook*. Blackwell Publishing Ltd.,
- 6 Oxford, 2005, pp.147-181.
- 7
- 8 37. J. Meija, L. Yang, Z. Mester and B.E. Sturgeon, *Isotopic analysis*. Wiley-VCH Verlag GmbH &
- 9 Co, KGaA, 2012, pp. 113-137
- 10
- 11 38. X.F. Sun, B.T.G. Ting, S.H. Zeisel and M. Janghorbani, *Analyst*, 1987, **112**, 1223-1228.
- 12
- 13 39. H. Vanhoe, C. Vandecasteele, J. Versieck, R. Dams, *Anal. Chim. Acta*, 1991, **244**, 259-267.
- 14
- 15 40. D. C. Grégoire, B. M. Acheson and R. P. Taylor, *J. Anal. At. Spectrom.*, 1996, **11**, 765-772.
- 16
- 17 41. Košler, M. Kučera and P. Sylvester, *Chem. Geol.*, 2001, **181**, 169-179.
- 18
- 19 42. S. Misra and P.N. Froelich. *J. Anal. At. Spectrom.*, 2009, **24**, 1524-1533.
- 20
- 21 43. G.D. Flesh, A.R. Anderson and H.J. Svec, *Int. J. Mass Spectrom.*, 1973, **12**, 265-272.
- 22
- 23 44. T. Magna, U.H. Wiechert and A.N. Halliday, *Int. J. Mass Spectrom.*, 2004, **239**, 67-76.
- 24
- 25 45. Y. Hu, X.Y. Chen, Y.K. Xu and F.Z. Teng, *Chem. Geol.*, 2018, **493**, 100-108.
- 26
- 27 46. H. Chen, Z. Tian, B. Tuller-Ross, R.L. Korotev and K. Wang. *J. Anal. At. Spectrom.*, 2019.
- 28 DOI: 10.1016/j.chemgeo.2019.04.028.
- 29
- 30 47. Y. Nishio and S.I. Nakai, *Anal. Chim. Acta*, 2002, **456**, 271-281.
- 31
- 32 48. Y. Gao, Y and J.F. Casey, *Geostand. Geoanal. Res.*, 2012, **36**, 75-81.
- 33
- 34 49. R.S. Hindshaw, R. Tosca, T.L. Goût, I. Farnan, N.J. Tosca, E.T. Tipper, *Geochim. Cosmochim.*
- 35 *Acta*, 2019, **250**, 219-237.
- 36
- 37 50. R.H. James and M.R. Palmer, *Chem. Geol.*, 2000, **166**, 319-326.
- 38
- 39 51. T.T. Phan, R.C. Capo, B.W. Stewart, G.L. Macpherson, E.L. Rowan and R.W. Hammack,
- 40 *Chem. Geol.*, 2016, **420**, 162-179.
- 41
- 42 52. Y. Huh, L.H. Chan, L. Zhang and J.M. Edmond, *Geochim. Cosmochim. Acta*, 1998, **62**, 2039-
- 43 2051.
- 44
- 45 53. L.H. Chan and J.M. Edmond, *Geochim. Cosmochim. Acta*, 1988, **52**, 1711-1717.
- 46
- 47 54. R. Millot, C. Guerrot and N. Vigier, *Geostand. Geoanal. Res.*, 2004, **28**, 153-159.
- 48
- 49 55. M.S. Choi, H.S. Shin and Y.W. Kil, *Microchem. J.*, 2010, **95**, 274-278.
- 50
- 51 56. S. Pfister, R.C. Capo, B.W. Stewart, G.L. Macpherson, T.T. Phan, J.B. Gardiner, J.R. Diehl,
- 52 C.L. Lopano and J.A. Hakala, *Appl. Geochem.*, 2017, **87**, 122-135.
- 53
- 54 57. N. Dauphas, A. Pourmand and F.Z. Teng, *Chem. Geol.*, 2009, **267**, 175-184.
- 55
- 56 58. F.Z. Teng and W. Yang, *Rapid Commun. Mass Spectrom.*, 2014, **28**, 19-24.
- 57
- 58 59. Thermo Finnigan Report NEPTUNE Thermo Finnigan Application Flash Report, 2001, No.
- 59 N2, 2p.
- 60

- 1  
2  
3 60. L.H. Chan and F.A. Frey, *Geochem. Geophys. Geosyst.*, 2003, **4**, 8707.  
4  
5 61. T. Elliott, A. Thomas, A. Jeffcoate and Y. Niu, *Nature*, 2006, **443**, 565.  
6  
7 62. P.A.P. Pogge von Strandmann, K.W. Burton, R.H. James, P. van Calsteren and S.R. Gislason,  
8 *Chem. Geol.*, 2010, **270**, 227-239.  
9  
10 63. H.M. Seitz, G.P. Brey, Y. Lahaye, S. Durali and S. Weyer, *Chem. Geol.*, 2004, **212**, 163-177.  
11  
12 64. L.H. Chan, W.P. Leeman and C.F. You, *Chem. Geol.*, 2002, **182**, 293-300.  
13  
14 65. H. Sun, Y. Gao, Y. Xiao, H.O. Gu and J.F. Casey, *Chem. Geol.*, 2016, **439**, 71-82.  
15  
16 66. G.L. Macpherson, R.C. Capo, B.W. Stewart, T.T. Phan, K. Schroeder and R.W. Hammack,  
17 *Geofluids*, 2014, **14**, 419-429.  
18  
19  
20  
21  
22  
23  
24  
25  
26  
27  
28  
29  
30  
31  
32  
33  
34  
35  
36  
37  
38  
39  
40  
41  
42  
43  
44  
45  
46  
47  
48  
49  
50  
51  
52  
53  
54  
55  
56  
57  
58  
59  
60

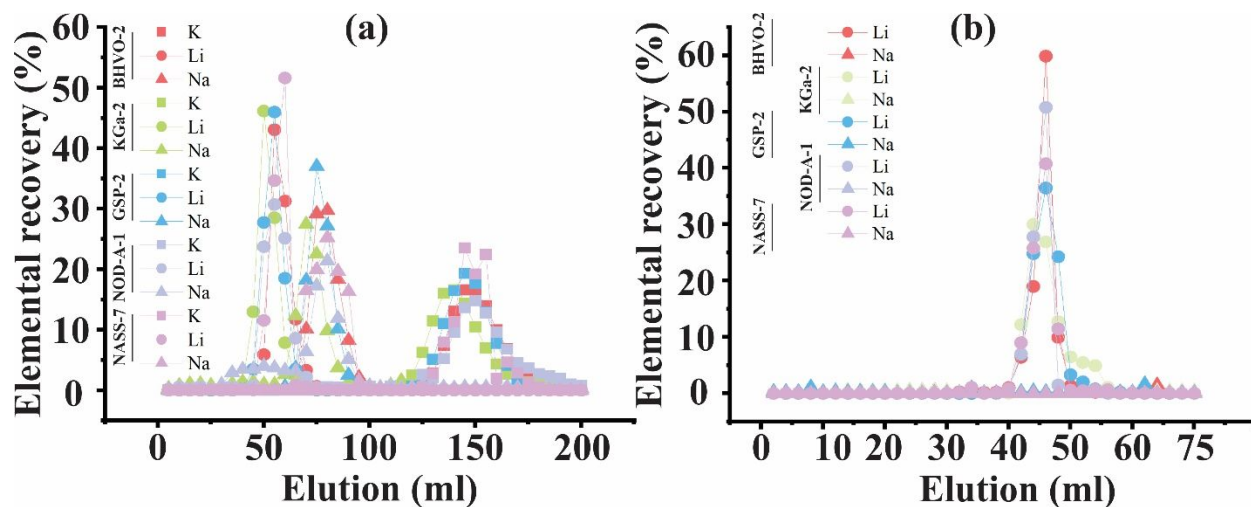


**Figure 1.** Column elution curves for multiple geostandards. (a) fat column 1 in 0.7 mol/L HNO<sub>3</sub>; (b) thin column 2 in 0.2 mol/L HCl. See text for details.

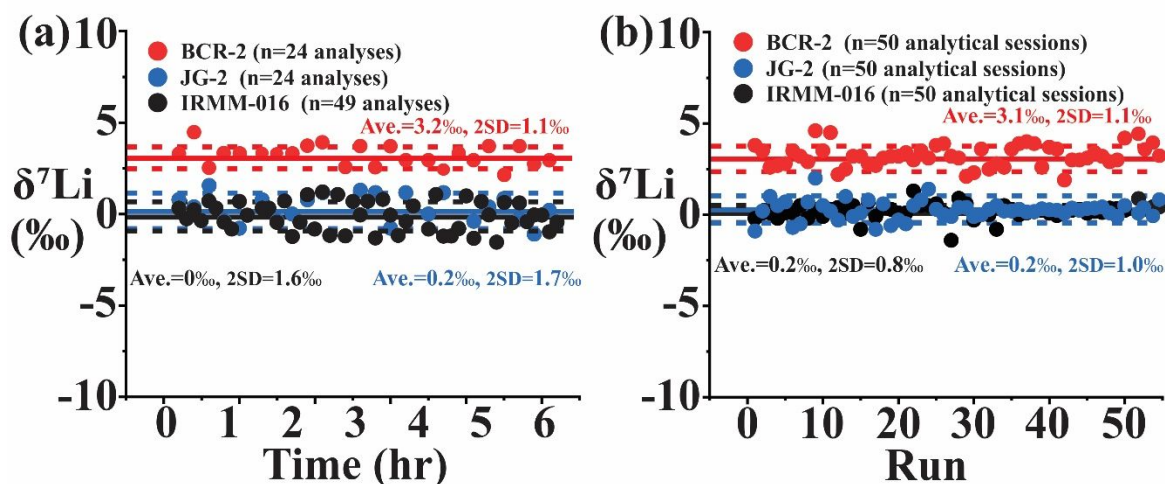


**Figure 2.** Short-term (a) and long-term (b) instrument stability and precision of Li isotopic analysis ( $\delta^7\text{Li}$ ) with respect to the IRMM-016 Li carbonate standard and igneous geostandards (BCR-2 and JG-2) purified through column chemistry. The instrumental stability determined by back-to-back runs of 0.5 ppb IRMM-016 in 2%  $\text{HNO}_3$  (v/v). The dashed lines represent the 2SD uncertainty of multiple sample measurements in short-term (~6 h) and long-term (10 months) as expected external precision. The solid lines represent the average value of multiple sample measurements. The long-term external precision (2SD) of the instrument is 0.8 ‰ for IRMM-016 Li reference, and 1.0 ‰ and 1.1 ‰ for BCR-2 basalt standard and JG-2 granite standard, respectively.



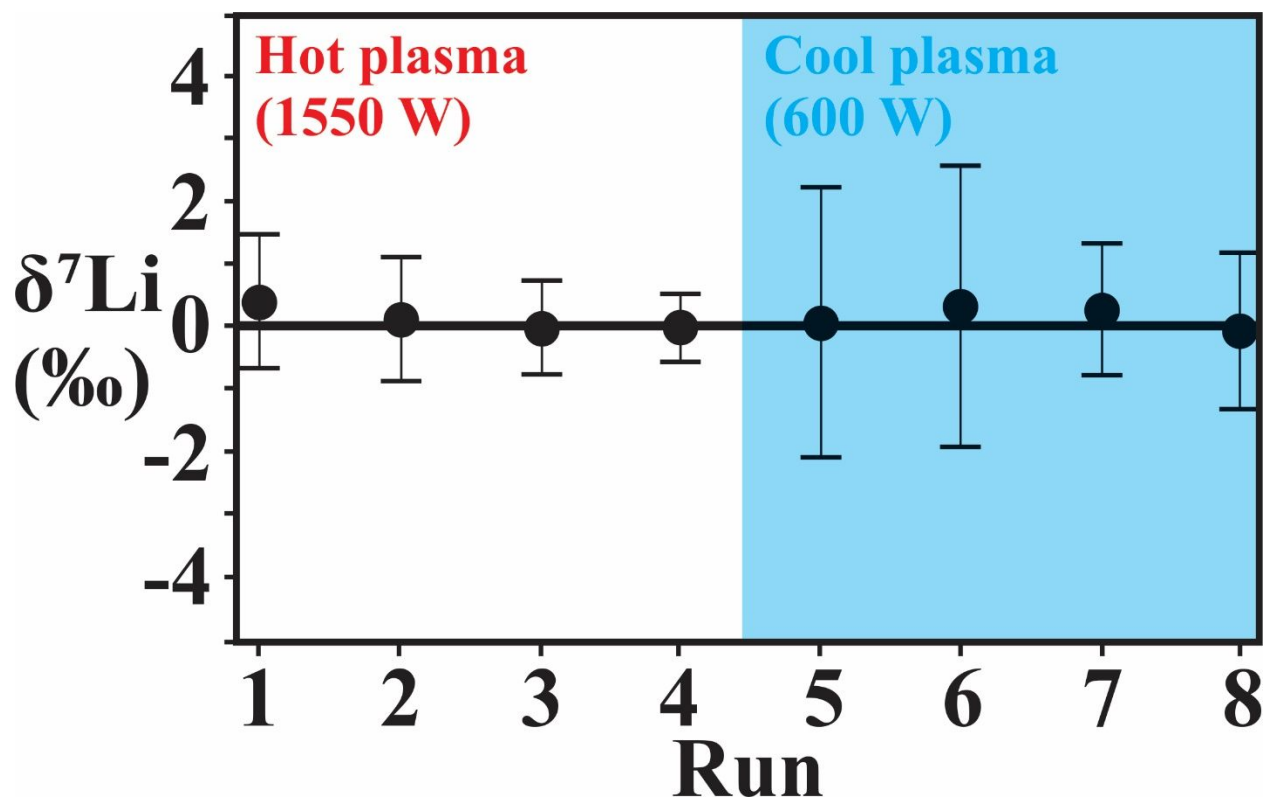


**Figure 3.** Multiple analyses on pure Li solutions (IRMM-016, 0.5 ppb Li) in hot (1550 W) and cool (600W) plasma conditions. The solid line stands for the expected the IRMM-016  $\delta^7\text{Li} = 0\%$ . Error bars represent the analytical uncertainty (2SD) of more than five repeated sample analyses.

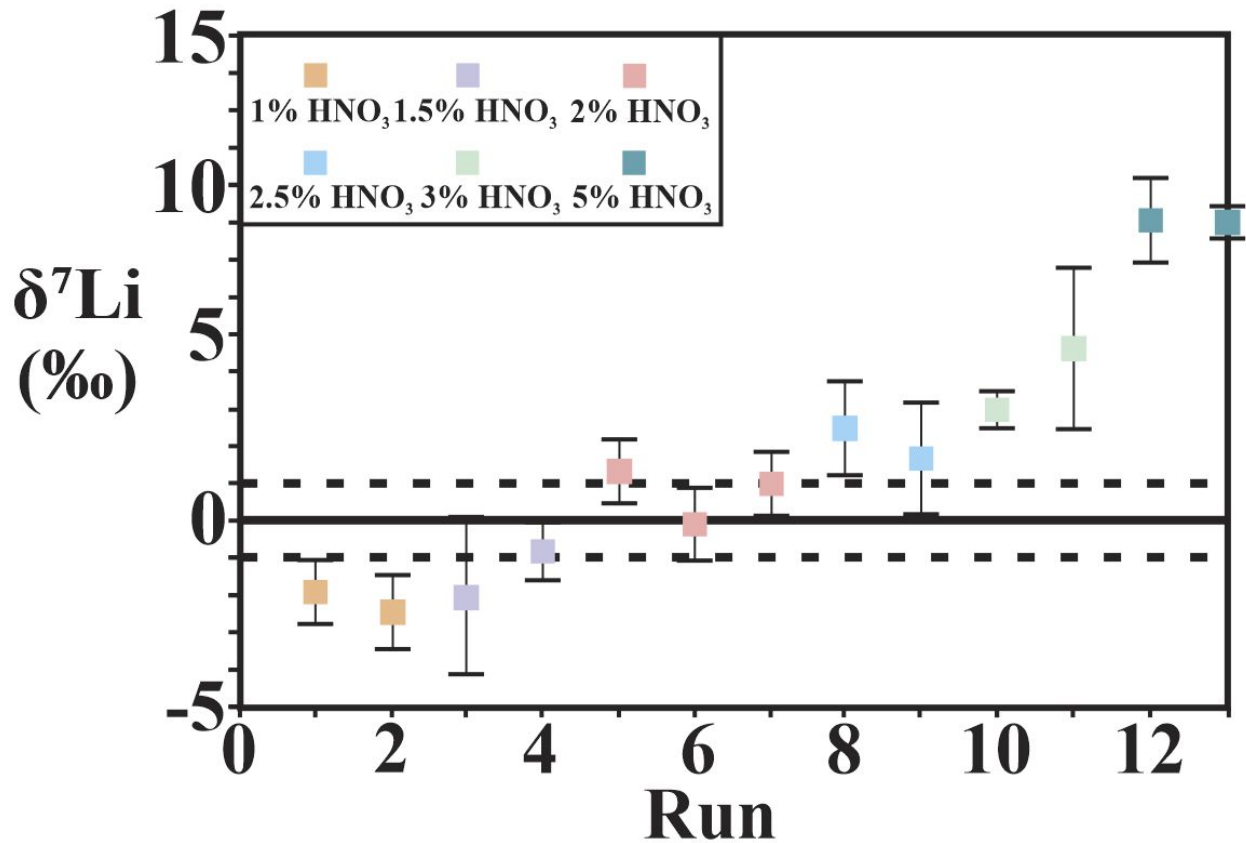


**Figure 4.** Effects of acid molarity mismatches on Li isotopic measurement by Q-ICP-MS. All measurements were bracketed by 0.5 ppb Li standard IRMM-016 in 2% HNO<sub>3</sub> (v/v). The solid line stands for the expected the IRMM-016  $\delta^7\text{Li}$  = 0 ‰. The dashed lines represent the long-term 2SD of multiple sample measurements as external precision. Error bars represent the analytical uncertainty (2SD) of more than five repeated sample analyses.

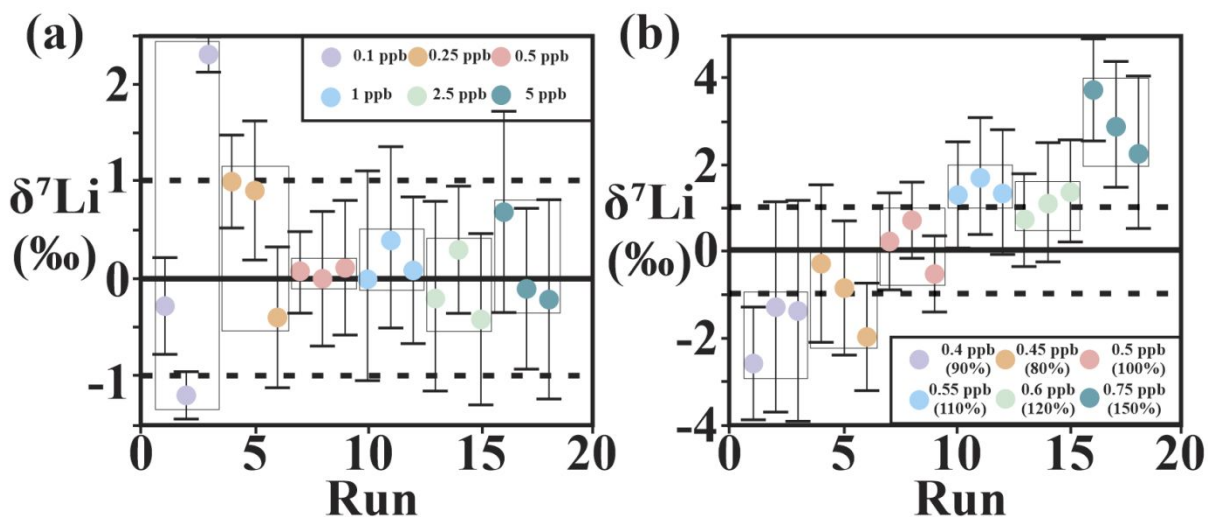


**Figure 5.** Effects of (a) Li concentrations and (b) concentration mismatch between aliquots and bracketing standards on Li isotopic measurement by Q-ICP-MS. The Li concentrations of samples and standards are controlled at 0.5 ppb and within 5% for all measurements conducted to ensure precision and accuracy. The solid line stands for the expected IRMM-016  $\delta^7\text{Li} = 0$  ‰. The dashed lines represent the long-term 2SD of multiple sample measurements as external precision. Error bars show the analytical uncertainty (2SD) of over five repeated sample analyses.

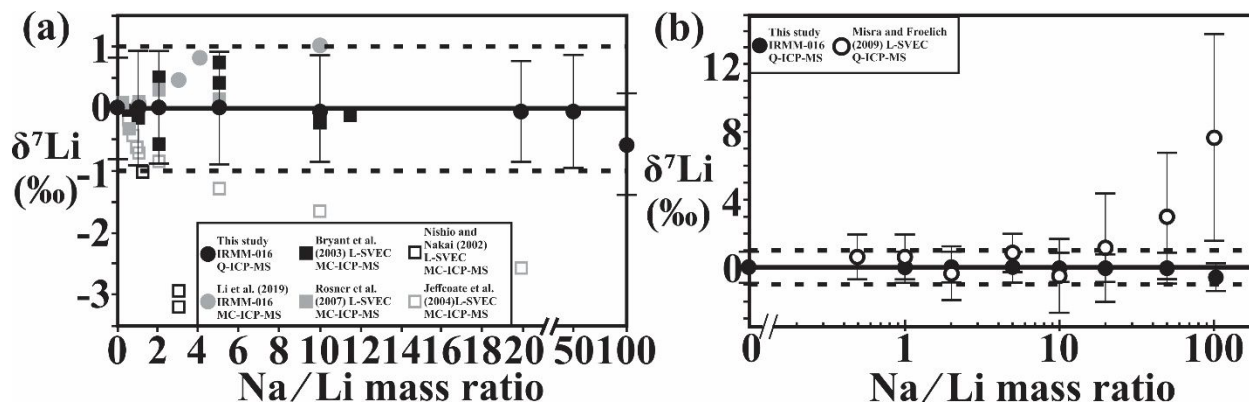


**Figure 6.** Assessment of the influence of Na on Li isotopic measurements with Na:Li molar ratios varying from 0 to 100. (a) Comparison between Q-ICP-MS and MC-ICP-MS data. (b) Comparison of Q-ICP-MS data reported in Misra and Froelich (2009) and this study. The  $\delta^7\text{Li}$  data was the average value of over five replicate analyses. The solid line stands for the IRMM-016  $\delta^7\text{Li} = 0$  ‰. The dashed lines represent the long-term 2SD of sample analysis by Q-ICP-MS. Error bars represent the analytical uncertainty (2SD) of over five repeated sample analyses. Some uncertainties of referential data of MC-ICP-MS methods are not shown.

**Table 1.** Two-step chromatographic Li purification protocols.

Details	Column 1	Column 2
Parameters	Fat column (ID=1.5 cm, polypropylene, BioRad™ Econo-Pac) filled with 17 mL AG50-X8 200-400 mesh cation-exchange resin (wet).	Thin column (ID=0.6 cm, polypropylene, custom-made ) filled with 3.4 mL AG50-X8 200-400 mesh cation-exchange resin (wet).
Loading capacity	29.6 meq	5.9 meq
Resin cleaning	100 mL 6 mol/L HCl	50 mL 6 mol/L HCl
Conditioning	50 mL 0.7 mol/L HNO <sub>3</sub>	20 mL 0.2 mol/L HCl
Sample loading	The samples are digested in 2.1 mL 0.7 mol/L HNO <sub>3</sub> . After centrifuging the solution, load 2 mL supernatant onto the fat columns.	The samples are digested in 2 mL 0.2 mol/L HCl. And then load onto the thin columns.
Matrix elution	25 mL 0.7 mol/L HNO <sub>3</sub>	30 mL 0.2 mol/L HCl
Pre-cut	5 mL 0.7 mol/L HNO <sub>3</sub> to monitor Li recovery	2 mL 0.2 mol/L HCl to monitor Li recovery
Li Collection	50 mL 0.7 mol/L HNO <sub>3</sub>	28 mL 0.2 mol/L HCl
Post-cut	5 mL 0.7 mol/L HNO <sub>3</sub> to monitor Li recovery	2 mL 0.2 mol/L HCl to monitor Li recovery
Resin regeneration	50 ml 6 mol/L HCl 50 ml MQ water	50 ml 6 mol/L HCl 50 ml MQ water

**Table 2.** Instrumental operating conditions and data acquisition parameters.

Equipment model	Agilent Technologies™ 7900 (this study)	Agilent Technologies™ 7500cs (Misra and Froelich, 2009) <sup>52</sup>
<b>Instrumental operating conditions</b>		
RF power (W)	1550 (hot plasma)	600 (Cool plasma)
RF matching (V)	1.58	-
Nebulizer	Concentric (PFA) self aspirating	Concentric (PFA) self aspirating
Sample uptake rate (μl/min)	~200 μL/min	~100 μl/min
Guard electrode	On	-
Sampling depth (mm)	6.8	6.5 to 7.5
Spray chamber	Quartz	Quartz
Spray chamber temperature (°C)	2	2
Cool Ar gas flow rate (L min <sup>-1</sup> )	15	-
Carrier Ar gas flow rate (L min <sup>-1</sup> )	0.95	0.60 to 0.65
Makeup Ar gas flow rate (L min <sup>-1</sup> )	0.35	0.30 to 0.40
Sampler cone	Nickel	Platinum
Skimmer cone	Nickel	Platinum
1st Extraction lens (V)	-110	-120 to -130
2nd Extraction lens (V)	-116.5	-10 to -5
Omega Lens (V)	7.8	-
Omega Bias (V)	-19	-
Integration time (s)	13s ( <sup>6</sup> Li) and 1s ( <sup>7</sup> Li)	13s ( <sup>6</sup> Li) and 1s ( <sup>7</sup> Li)
Nebulizer pump (rps)	0.1	/
Sample uptake time (s)	45	60
Stabilize time (s)	30	-
Measurement time (s)	50	-
Pulse detection limit (cps)	1.0 × 10 <sup>6</sup>	3.0 × 10 <sup>6</sup>
Wash-out time (s)	180 (Rinse 1: 75; Rinse 2: 45; Rinse 3: 60)	240

**Table 3.** Lithium recovery and Na/Li ratios before and after isolation of thirteen geostandards.

Seperation method	Sample	type	Li mass added (ng)	Li mass collection (ng)	Li recovery (%)	Final Na/Li mass ratio
Dual-column chromatography	NIST-SRM-1d	limestone	84.4	83.2	98.6	0.4
	JCP-1	Coral	40.6	40.8	100.5	0.3
	GSP-2	Granodiorite	649.2	651.0	100.3	0.1
	BHVO-2	Basalt	70.0	69.8	99.7	0.9
	BCR-2	Basalt	81.0	82.0	101.2	0.3
	JB-2	Basalt	488.6	487.8	99.8	0.4
	JG-2	Granite	423.2	423.0	100.0	0.5
	KGa-2	Clay (kaolinite)	351.2	347.6	99.0	0.1
	Swy-3	Clay (smectite)	371.8	367.0	98.7	0.0
	IMt-2	Clay (illite)	307.0	308.2	100.4	0.5
	SBC-1	Shale	1084.6	1078.8	99.5	0.1
	NASS-7	Seawater	919.0	913.6	99.4	1.0
	NOD-A-1	Marine Mn nodules	713.4	720.4	101.0	0.3

**Table 4.** Measured Li isotope ratios and reported data in reference materials.

Reference material	Type	Source	Reference	$\delta^7\text{Li}$ (‰)	2SD	Instrument	Reference material	Source	Reference	$\delta^7\text{Li}$ (‰)	2SD	Instrument	
BHVO-1	Basalt	USGS	50	5.8	/	TIMS	JG-2	Granite	GSJ	34	0.15	0.15	MC-ICP-MS
BHVO-1			59	4.61	/	MC-ICP-MS	JG-2			51	0	0.2	MC-ICP-MS
BHVO-1			60	5.2	/	TIMS	JG-2			27	0.24	0.2	MC-ICP-MS
BHVO-1			6	5.5	0.6	MC-ICP-MS	JG-2			6	-0.7	0.4	MC-ICP-MS
BHVO-1			6	4.7	0.4	MC-ICP-MS	JG-2			50	0.4	0.1	TIMS
BHVO-1			10	5	1.5	MC-ICP-MS	JG-2			35	0.32	0.31	MC-ICP-MS
BHVO-1			7	4.3	/	MC-ICP-MS	JG-2			This study	0.25	1.02	Q-ICP-MS
BHVO-2			28	4.68	0.16	MC-ICP-MS	GSP-2			34	-0.78	0.25	MC-ICP-MS
BHVO-2			34	4.5	0.24	MC-ICP-MS	GSP-2			65	-0.8	0.3	MC-ICP-MS
BHVO-2			30	4.46	0.37	MC-ICP-MS	GSP-2			35	-0.56	0.55	MC-ICP-MS
BHVO-2			27	4.66	0.22	MC-ICP-MS	GSP-2			This study	-0.56	0.72	Q-ICP-MS
BHVO-2			48	4.29	0.23	MC-ICP-MS	IRMM-016			34	0	0.16	MC-ICP-MS
BHVO-2			29	4.63	0.16	MC-ICP-MS	IRMM-016			56	0.2	0.3	MC-ICP-MS
BHVO-2			61	4.8	0.3	MC-ICP-MS	IRMM-016			66	0.1	0.4	MC-ICP-MS
BHVO-2			62	4.9	0.8	MC-ICP-MS	IRMM-016			51	0.2	0.2	MC-ICP-MS
BHVO-2	35	4.63	0.29	MC-ICP-MS	IRMM-016	54	0.2	0.24	MC-ICP-MS				
BHVO-2	This study	4.7	0.57	Q-ICP-MS	IRMM-016	27	0.14	0.04	MC-ICP-MS				
BCR-1	Basalt	USGS	51	2.5	0.5	MC-ICP-MS	IRMM-016	This study	0.16	0.83	Q-ICP-MS		
BCR-1			44	2.38	0.52	MC-ICP-MS	NASS-5	30	30.55	0.45	MC-ICP-MS		
BCR-1			17	2	0.7	MC-ICP-MS	NASS-5	55	30.29	0.65	MC-ICP-MS		
BCR-2			30	2.84	0.45	MC-ICP-MS	NASS-5	28	30.64	0.44	MC-ICP-MS		
BCR-2			28	2.87	0.39	MC-ICP-MS	NASS-5	29	30.72	0.17	MC-ICP-MS		
BCR-2			29	2.6	0.3	MC-ICP-MS	NASS-6	34	30.87	0.15	MC-ICP-MS		
BCR-2			31	2.82	0.13	MC-ICP-MS	NASS-6	56	29.6	2.2	MC-ICP-MS		
BCR-2			35	3.02	0.51	MC-ICP-MS	NASS-6	62	31.3	0.9	MC-ICP-MS		
BCR-2			This study	3.16	1.1	Q-ICP-MS	NASS-7	35	30.42	0.97	MC-ICP-MS		
JB-2			Basalt	GSJ	24	4.9	0.7	TIMS	NASS-7	This study	30.63	1.31	Q-ICP-MS
JB-2					25	5.1	1.2	MC-ICP-MS	NIST-SRM-1d	35	5.63	0.48	MC-ICP-MS
JB-2					50	6.8	/	TIMS	NIST-SRM-1d	This study	6.07	1.2	Q-ICP-MS
JB-2					47	4.3	0.3	MC-ICP-MS	JCP-1	29	20.16	0.2	MC-ICP-MS
JB-2					6	3.9	0.4	MC-ICP-MS	JCP-1	31	20.27	0.41	MC-ICP-MS
JB-2					14	4.7	/	MC-ICP-MS	JCP-1	35	19.56	0.53	MC-ICP-MS
JB-2	27	4.3			0.26	MC-ICP-MS	JCP-1	This study	19.83	1.07	Q-ICP-MS		
JB-2	44	4.7			0.29	MC-ICP-MS	NOD-A-1	35	26.31	0.97	MC-ICP-MS		
JB-2	7	4			/	MC-ICP-MS	NOD-A-1	This study	26.85	1.3	Q-ICP-MS		
JB-2	63	5.2			/	MC-ICP-MS	Swy-1	18	5.9	/	MC-ICP-MS		
JB-2	29	4.31			0.69	MC-ICP-MS	Swy-3	This study	-0.58	0.36	Q-ICP-MS		
JB-2	64	5.1			0.4	TIMS	KGa-2	18	0.1	/	MC-ICP-MS		
JB-2	35	4.71			0.23	MC-ICP-MS	KGa-2	35	0.15	0.04	MC-ICP-MS		
JB-2	This study	4.56			0.56	Q-ICP-MS	KGa-2	This study	0.16	0.69	Q-ICP-MS		
SBC-1	Shale	USGS			35	0.29	0.03	MC-ICP-MS	IMt-1	18	2.5	/	MC-ICP-MS
SBC-1			This study	0.23	0.9	Q-ICP-MS	IMt-2	This study	5.95	0.68	Q-ICP-MS		